Comparison of Linear State Signal Shaping Model Predictive Control with Classical Concepts for Active Power Filter Design

Kathrin Weihe[1,2], Carlos Cateriano Yáñez[1,2], Georg Pangalos[1] and Gerwald Lichtenberg[2]
[1]*Application Center Power Electronics for Renewable Energy Systems, Fraunhofer Institute for Silicon Technology ISIT, Steindamm 94, 20099 Hamburg, Germany*
[2]*Faculty Life Sciences, Hamburg University of Applied Sciences, Ulmenliet 20, 21033 Hamburg, Germany*
{*kathrin.weihe, carlos.cateriano.yanez, georg.pangalos*}*@isit.fraunhofer.de*, {*kathrinjoungah.weihe, carlos.caterianoyanez,*

Keywords: Model Predictive Control, Active Power Filter.

Abstract: Many power networks are currently under major change processes due to the necessary integration of renewable energy sources. This brings the need to include Active Power Filter (APF) as well as controlling them in an adequate way. New control concepts like Linear State Signal Shaping Model Predictive Control (LSSS MPC) are specialized for these tasks and complex compared to classical concepts. Simulation studies show the advantages of LSSS MPC in performance, robustness and Total Harmonic Distortion (*THD*) compensation.

1 INTRODUCTION

The amount of higher order harmonics is increasing in the electrical grid, due to the increasing share of sources and loads connected via power converters, (Liang, 2016). Solar panels use switch-mode inverters to feed energy into the grid with switching frequencies of about 20 kHz (Mohan et al., 2003). Even with such high frequencies a perfect sine wave can not be generated, i.e. harmonics are introduced. This holds true not only for sources but also for loads. One possibility to cope with this problem is to use active power filters (APF) to compensate the harmonics, (Kumar and Mishra, 2016).

Security and reliability aspects have a strong focus in power grids, such that a test of a new concept of compensating harmonics is not performed without substantial evidence of its functionality, e.g. given by appropriate simulation studies. In this paper, a novel controller is compared to one of the well established and commonly used controllers by closed loop simulations within a standard benchmark grid. Since the focus of the simulation is to analyse the feasibility of the new controller, the models involved for the grid are of low complexity, thus enabling an easier analysis of the controller response.

The most established power control theories for APF reference current generation are: Instantaneous Symmetrical Component (ISC), Instantaneous Reactive Power (IRP) and Synchronous Reference Frame (SRF). The ISC theory relies on the transformation of the instantaneous supply voltages and load currents, that for unbalanced or distorted supply voltage conditions refers to the positive sequence components of the supply voltage for the calculation of the reference current components. On the IRP or p-q theory, the Clarke transformation is used for the translation of the instantaneous supply voltages and load currents into the $\alpha - \beta$ frame, where the compensation currents are generated and then transformed back for implementation. The SRF or d-q theory relies on the $dq0$ transformation for the load currents, which involves the calculation of the phase θ through a phase locked loop (PLL), that once in the $dq0$ domain are used to compute the reference currents, followed by an inverse transformation (Kumar and Mishra, 2016).

The strategy proposed in this paper relies on a novel control approach by a Linear State Signal Shaping Model Predictive Control (LSSS MPC) as introduced in (Cateriano Yáñez et al., 2018). This theory establishes that if a desired behaviour of a dynamical linear system lies in a linear signal shape class, a reformulated linear Model Predictive Control (MPC) can be used to ensure that state signals are driven into this class.

The simulation analysis in this paper aims to compare this new control concept against the well established p-q theory. For this purpose, the paper is struc-

Weihe, K., Yáñez, C., Pangalos, G. and Lichtenberg, G.
Comparison of Linear State Signal Shaping Model Predictive Control with Classical Concepts for Active Power Filter Design.
DOI: 10.5220/0006910401670174
In *Proceedings of 8th International Conference on Simulation and Modeling Methodologies, Technologies and Applications (SIMULTECH 2018)*, pages 167-174
ISBN: 978-989-758-323-0

tured as follows. In section 2 the main features of the grid model and the reference current generation principles are presented, whereas in section 3, the two control approches are introduced. Section 4 presents the simulation results and analysis. Finally, section 5 gives a summary and draws conclusions from the simulation study. A recapitulation of MPC as well as LSSS MPC is given in the Appendix.

2 GRID MODEL

This chapter introduces the models used for the comparative simulation of APF control methods. Starting from a general definition of state space models the grid model as well as a single phase equivalent representation are given. The section is concluded by an analysis of the disturbance signal.

2.1 State Space Models

The dynamics of a linear system can be represented by a continuous-time state space model

$$\dot{\mathbf{x}}(t) = \mathbf{A}_c\mathbf{x}(t) + \mathbf{B}_c\mathbf{u}(t)\,, \tag{1}$$

where the variable t is time, the vector $\mathbf{x} \in \mathbb{R}^n$ refers to the state, vector, $\mathbf{u} \in \mathbb{R}^m$ to the input vector, $\mathbf{A}_c \in \mathbb{R}^{n\times n}$ to the system matrix, and $\mathbf{B}_c \in \mathbb{R}^{n\times m}$ to the input matrix.

Introducing fixed sampling times t_s taken at $t = kt_s$ for $k = 0,1,2,\ldots$, the model (1) can be rewritten as discrete state space model

$$\mathbf{x}(k+1) = \mathbf{A}\mathbf{x}(k) + \mathbf{B}\mathbf{u}(k)\,, \tag{2}$$

with appropriate matrices $\mathbf{A} \in \mathbb{R}^{n\times n}$ and $\mathbf{B} \in \mathbb{R}^{n\times m}$.

2.2 System Description

A simulation of a three-phase three-node grid model consisting of a three-phase diode rectifier acting as a non-linear load is used to evaluate the proposed new control method to compensate current harmonics with. Active power filters can be connected in series or in parallel (shunt) to the load, with series APF being suitable for power quality improvement, (Hashim et al., 2016) while shunt APF are used to provide reactive power and current harmonics compensation, (Akagi, 2005).

Figure 1 shows the electrical circuit configuration of the simulation setup. The grid model uses a balanced supply of 230 V root mean square (RMS) phase-to-ground voltage with a frequency of 50 Hz, hence a shunt configuration for the APF is chosen. Active filter configurations most commonly consist of a three-phase voltage-source pulse width modulation converter (VSC) utilizing a DC link capacitor as voltage supply, a coupling inductor to filter switching ripples and a controller. The filter detects the instantaneous load current i_l and applies the compensating current i_f at the point of common coupling (PCC) to cancel out harmonics.

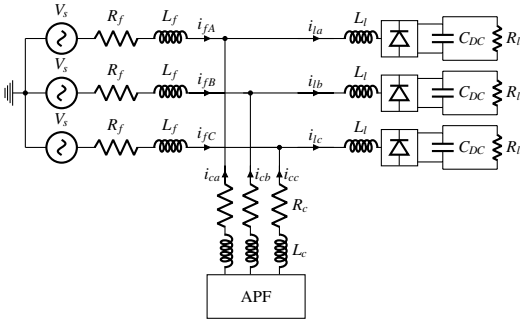

Figure 1: Three-phase three-node grid model.

2.3 Single Phase Equivalent Circuit

The system behaviour can approximately be modelled as a current source providing non-linear currents to the grid which leads to the single phase equivalent circuit shown in Figure 2. The non-linear load is represented by an uncontrollable current source, the APF acts as controllable current source, and the supply is modelled by a voltage source. The non-linear load is connected to the supply voltage by a feeder line with the resistance R_f and the inductance L_f respectively, which generate a voltage drop v_l over the feeder line. To reduce modelling complexity the LSSS MPC employs a state space model of the single phase equivalent circuit to calculate the compensation current.

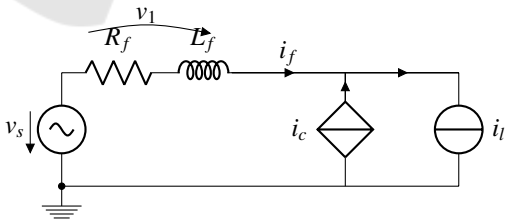

Figure 2: Single phase equivalent circuit of a shunt active filter compensating a non-linear load.

The model has the state vector:

$$\mathbf{x} = \begin{pmatrix} v_l & \frac{di_c}{dt} & \frac{di_l}{dt} \end{pmatrix}^\mathsf{T} \in \mathbb{R}^3 \tag{3}$$

with the control input $u(t) = \frac{\mathrm{d}^2 i_c}{\mathrm{d}t^2} \in \mathbb{R}$ and the distur-

bance $d(t) = \frac{d^2 i_l}{dt^2}$. The state space model is given as

$$\frac{dx_1}{dt} = -R_f\, x_2 + R_f\, x_3 - L_f\, u(t) + L_f\, d(t) \quad (4)$$

$$\frac{dx_2}{dt} = u(t) \quad (5)$$

$$\frac{dx_3}{dt} = d(t) \quad (6)$$

where (4) can be derived by Kirchhoff's circuit laws. In order to gain access to the feeder line voltage v_l as state, an augmented state space model is derived with additional states in (5) and (6). Note, that this leads to a reformulation of the original input i_c and disturbance i_l.

2.4 Disturbance Signal

The non-linear load current i_l is modelled as an ideal current source acting as a disturbance $d(t)$ to the single phase state space model as shown in figure 2. In order to generate the disturbance, a physical model of a diode rectifier is simulated as part of the grid model shown in figure 1. Due to the nature of the diodes included, a non-linear current-voltage characteristic can be observed when using a bridge rectifier. Although methods exist to obtain a state space model for such devices (Emadi, 2001), simulation tools like MATLAB SIMULINK have the great advantage of providing transient analysis of power electronics without the need to perform the complex modelling process.

In this paper the grid model including the rectifier is built using SIMULINK models. The current load drawn by the rectifier is measured and fed in to the state space model which affects the calculation of the compensation current generated by the controller, effectively affecting back the physical model of the rectifier in the grid. Thus the measurement of the disturbance is constantly updated by the simulation of the physical diode rectifier model.

3 CONTROLLER MODELS

To achieve good harmonic compensation, APF need to detect the harmonic content drawn from the load in order to inject the inverse equivalent as compensation current into the PCC. Conventional APF use high pass filter to extract harmonics from the load current. High performance digital signal processors (DSPs), field-programmable gate arrays (FPGAs) together with high precision current and voltage measurement devices need to be utilized to guarantee as little errors in current detection as possible, as errors and delays can reduce the performance of the APF or even evoke instability (Malesani et al., 1998).

In contrast to this, the LSSS MPC does not rely on a high pass filter but instead uses a linear shape class defining a fundamental harmonic condition to calculate a compensation current which is able to obtain a sinusoidal signal, see section 3.2.

3.1 Classical Control for Shunt APF

Among a wide range of methods to calculate the reference compensation current, the instantaneous active and reactive power theory (p-q theory) (Akagi et al., 1986) has proven to provide good harmonic compensation performance both in simulation and application (Akagi, 2005). The PCC voltages and load currents are transformed into the $\alpha - \beta$ orthogonal frame using the Clarke transformation defined as

$$\begin{pmatrix} v_\alpha \\ v_\beta \end{pmatrix} = \sqrt{\frac{2}{3}} \begin{pmatrix} 1 & -\frac{1}{2} & -\frac{1}{2} \\ 0 & \frac{\sqrt{3}}{2} & -\frac{\sqrt{3}}{2} \end{pmatrix} \begin{pmatrix} v_{fA} \\ v_{fB} \\ v_{fC} \end{pmatrix} \quad (7)$$

$$\begin{pmatrix} i_{l\alpha} \\ i_{l\beta} \end{pmatrix} = \sqrt{\frac{2}{3}} \begin{pmatrix} 1 & -\frac{1}{2} & -\frac{1}{2} \\ 0 & \frac{\sqrt{3}}{2} & -\frac{\sqrt{3}}{2} \end{pmatrix} \begin{pmatrix} i_{lA} \\ i_{lB} \\ i_{lC} \end{pmatrix}. \quad (8)$$

The instantaneous real power p_l and instantaneous imaginary power q_l are then calculated by

$$\begin{pmatrix} p_l \\ q_l \end{pmatrix} = \begin{pmatrix} v_\alpha & v_\beta \\ -v_\beta & v_\alpha \end{pmatrix} \begin{pmatrix} i_{l\alpha} \\ i_{l\beta} \end{pmatrix}. \quad (9)$$

Assuming a purely sinusoidal source voltage, both p_l and q_l can be separated into a DC and an AC component with the previous mentioned high pass filter, with the AC component referring to the amount of harmonic distortion incorporated in the load current. The reference compensation current $i_{c,ref}$ is generated by applying the inverse Clarke transformation to the AC component of p_l and q_l.

To induce the compensation current into the grid, a VSC controlled by a hysteresis band controller is used in this paper. The switching signals are generated by comparing the compensating current i_c with the reference current $i_{c,ref}$ and calculating the current error. If the error exceeds the upper or lower limit of a fixed hysteresis band, the legs of the VSC are switched accordingly, so the compensating current stays inside the hysteresis band (Buso et al., 1998).

It is worth mentioning, that while simple in implementation and robust in application, the hysteresis band controller produces varying switching frequencies, which can lead to unsatisfactory behaviour (Buso et al., 1998).

3.2 New Shape Class MPC Controller

The control focus of the APF of this implementation is the compensation of the *THD* on the feeder current i_f and the feeder voltage v_f, i.e leading them into the shape class of perfect fundamental harmonic functions. The property of this shape class can be expressed as the solution of the initial value problem of the homogeneous ordinary second order differential equation (ODE)

$$\frac{\mathrm{d}^2x(t)}{\mathrm{d}t^2} + (2\pi f)^2 x(t) = 0, \tag{10}$$

that leads to a sinusoidal state signal $x(t)$ with a fixed frequency f, zero offset, and an arbitrary amplitude, (Ahlfors, 1966).

In order to express the ODE in (10) as a linear shape class of the form (19) as given in the appendix, it needs to first be transformed into a discrete-time form. This can be achieved using forward numerical differentiation to approximate the second order derivative in (10), with a step size t_s and an accuracy order of $O(t_s^2)$, (Fornberg, 1988),

$$\frac{\mathrm{d}^2x(t)}{\mathrm{d}t^2} \approx \frac{2x(k) - 5x(k+1) + 4x(k+2) - x(k+3)}{t_s^2}, \tag{11}$$

that when replaced in (10) starting at discrete time $k+1$ (first future time step), leads to a linear shape class with $s = 1$, $n = 1$, and $T = 4$, defined by the row vector

$$\mathbf{v} = \frac{1}{t_2^2}\begin{pmatrix} 2 + (2\pi f t_s)^2 & 5 & 4 & -1 \end{pmatrix} \in \mathbb{R}^{1\times 4}. \tag{12}$$

Note that by using forward numerical differentiation the signal shape can be expressed by only using future state predictions which results in a homogeneous set-up for the **Q** weight matrix, while using a more precise centered approximation would require to modify the prediction horizon to include past states.

4 SIMULATION STUDIES

MATLAB SIMULINK is used to simulate the model in order to evaluate the performance and feasibility of the LSSS MPC method compared to the IRP method.

4.1 Parameter Settings

The simulation is run with a fixed-step solver with different fundamental sample times for the IRP APF and the LSSS MPC as explained in greater detail in section 4.2. Simulations showed that a first order Euler forward solver provides sufficient accuracy and is chosen over a higher order solver to improve simulation speed.

Table 1: Simulation parameters.

Parameter	Symbol	Value
Sampling time IRP APF	t_{s1}	1×10^{-6} s
Sampling time MPC APF	t_{s2}	2×10^{-5} s
Phase-to-ground RMS voltage	v_s	230 V
Grid frequency	f	50 Hz
Feeder line resistance	R_f	1 Ω
Feeder line inductance	L_f	0.01 mH
Filter coupling resistance	R_c	0.001 Ω
Filter coupling inductance	L_c	3.50 mH
VSC DC Link voltage	V_{DC}	700 V
AC load coupling inductance	L_l	2 mH
DC smoothing capacitor	C_{DC}	0.68 mF

Table 1 shows the parameters of the grid model. A bridge rectifier using a smoothing capacitor on the DC side is connected to every phase of the grid model, drawing non-linear currents. To analyse different load scenarios and transient behaviour of the APF, three different load steps are implemented. Starting from a 100 Ω resistance at the DC side of the rectifier, after a simulation time of 0.3 s the load resistance drops to 9 Ω and after a simulation time of 0.6 s to 2 Ω respectively to simulate an increase in load current drawn from the grid. The high pass filter for the classical IRP APF is designed using standard methods (Akagi et al., 1986). The DC link voltage of the VSC used to generate compensation currents is controlled by a PI-Controller that was tuned using the Ziegler-Nichols method (Ziegler and Nichols, 1942). Additionally, in order to enable the IRP APF to react on time to the changes in load current of the rectifier, an AC load coupling inductance L_l is needed in series between the rectifier and the PCC; this limitation is not present on the LSSS MPC, howerever is also included for simulation consistency.

The **Q** and **R** matrices are tuned heuristically, with the cost of control effort tuned to 8×10^3, the cost of control error is presented in table 2. Only the weight for the feeder line voltage is set to ensure a

Table 2: **Q** matrix tuning.

State	State weight
v_l	10^3
$\frac{di_c}{dt}$	0
$\frac{di_l}{dt}$	0

sinsudoidal signal shape, assuming this can only be achieved by sinusoidal feeder line current. The length of prediction horizon H_p and input horizon H_u are chosen to be equal to the number of samples in one period $\frac{1}{ft_{s2}}$. The controller updates once per period, in contrast to traditional MPC which updates once per sample. This means that the controller uses its full predicted optimal input and not only the first value as usual with the MPC. This update setup is chosen in accordance with the periodic behaviour of the target fundamental harmonic shape class.

4.2 Assumptions and Criteria

The LSSS MPC incorporates a model of the single phase equivalent circuit, so the controller is able to calculate the compensation current for one phase only. Both APF are connected to the three-phase three-node model, with the LSSS MPC being capable of providing compensation for one phase in the current state of development. To provide a comparable performance evaluation, the simulation results for one phase will be presented.

Also note, that an APF utilizing a hysteresis band controlled VSC is a source of harmonic currents itself by inducing the compensation current with a variable switching frequency. On the other hand, the LSSS MPC uses an ideal current source to generate the compensation current for the benefit of reduced modelling complexity. To provide an environment, where additional harmonic distortion due to the switching ripples of the VSC is minimized, a high sampling frequency of 100 kHz is chosen for the simulation of the IRP APF method as well as small upper and lower band limits of 0.01 A for the hysteresis controller.

In order to analyse the compensation performance, the total harmonic distortion *THD* is calculated by

$$THD = \frac{\sqrt{\sum_{n=2}^{\infty} X_n^2}}{X_1}, \tag{13}$$

where *THD* refers to the ratio of the RMS values of higher order harmonic frequencies X_n to the fundamental X_1, (Shmilovitz, 2005).

4.3 Results

As can be seen in figure 3 the classical APF using the IRP method generates a compensation current (mid plot) which leads to a nearly purely sinusoidal feeder line voltage (bottom plot) and current (top plot, red dashed line).

Similar results can be observed for the APF using the LSSS MPC, as shown in figure 4. However, a higher amplitude in the compensation current can be observed from the mid plot which can be interpreted as an excess of energy going into the load current (top plot, blue solid line). Also note, that there is a DC offset in the feeder current, which dissipates with longer simulation time and higher amount of harmonic distortion.

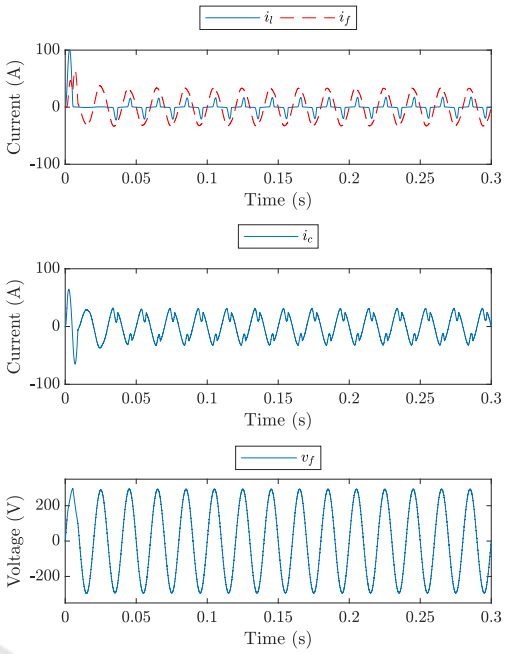

Figure 3: Simulation results for the load compensation using IRP APF.

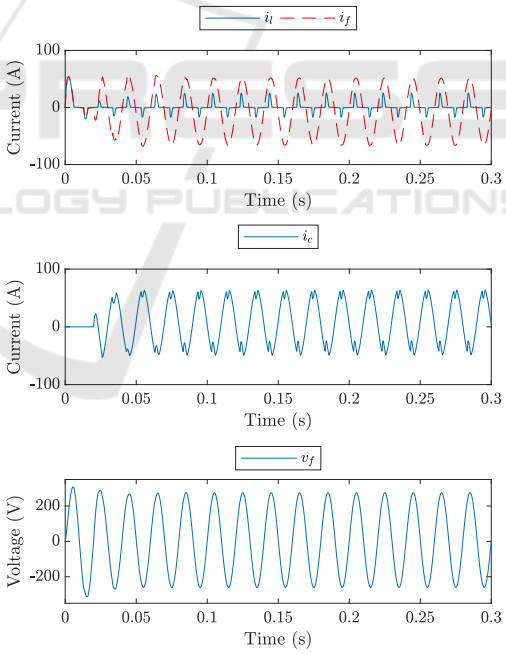

Figure 4: Simulation results for the load compensation using LSSS MPC APF.

Table 3: Simulation results for *THD* reduction of feeder line voltage and current.

	THD (v_f)		*THD* (i_f)	
Load scenario	IRP	MPC	IRP	MPC
100 Ω	0.65%	0.17%	4.35%	0.78%
9 Ω	0.45%	0.35%	0.75%	1.57%
2 Ω	1.15%	0.35%	3.75%	1.33%

Figure 5 shows the evolution of the feeder line voltage *THD* for the first load step for both compensation methods. While the IRP APF settles to a *THD* of 0.65% after around 0.05 s, the LSSS MPC continues to reduce the *THD* to 0.17%.

Table 3 shows the simulation results for the feeder line voltage and current *THD* reduction for the whole simulation time frame including the three different load scenarios. The LSSS MPC APF achieves better overall *THD* reduction of the feeder line voltage and current, adapting to the different load step changes. However, the IRP APF shows a better result for the feeder current only in the second load step scenario for which the AC load coupling inductance was specifically parametrized. It is important to notice that the LSSS MPC was only implicitly tuned to compensate the feeder voltage, which can explain its overall better performance on voltage against current *THD*.

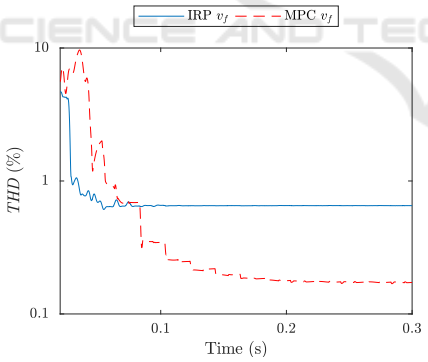

Figure 5: Dynamic behaviour of the *THD* reduction for the first load scenario.

5 CONCLUSIONS

This section summarises the paper and gives an outlook on future work.

5.1 Summary

A simulation testbench has been built to compare a novel LSSS MPC control method to a classical IRP APF approach. While the high pass filter on an IRP APF needs to be specifically designed to work in a given load scenario, the LSSS MPC through its cost function is capable of adapting to a wider variety of load scenarios. The simulation results show that an LSSS MPC approach has the potential to successfully control an APF. Since the LSSS MPC considers predictions of the disturbance one period ahead, it is more flexible to adapt to abrupt load changes, thus not actually needing an AC load coupling inductance which is the case for the IRP APF.

5.2 Outlook

While the LSSS MPC shows good overall compensation results in the simulated time frame, the observed excess in compensation current should be avoided to minimize the energy consumption of the APF. For longer simulation time the excess of energy can even keep building up. This can be addressed by applying a state constraint to the LSSS MPC, however this could lead to a higher computational effort. Additionally, to control both feeder line voltage and current, the cost function of the LSSS MPC would need to be adapted to penalize both states, thus leading to a more challenging tuning of the **Q** and **R** matrices. Applying constraints to the LSSS MPC as well as tuning the controller under more complex conditions is currently being researched.

ACKNOWLEDGEMENTS

This contribution was partly developed within the project NEW 4.0 (North German Energy Transition 4.0) which is funded by the German Federal Ministry for Economic Affairs and Energy (BMWI). This paper was also partly funded by the Free and Hanseatic City of Hamburg (Hamburg City Parliament publication 20/11568).

REFERENCES

Ahlfors, L. (1966). *Complex Analysis: An introduction to the theory of analytic functions of one complex variable*. Harvard University.

Akagi, H. (2005). Active Harmonic Filters. *Proceedings of the IEEE*, 93(12):2128–2141.

Akagi, H., Nabae, A., and Atoh, S. (1986). Control Strategy of Active Power Filters Using Multiple Voltage-Source PWM Converters. *IEEE Transactions on Industry Applications*, IA-22(3):460–465.

Buso, S., Malesani, L., and Mattavelli, P. (1998). Comparison of current control techniques for active filter applications. *IEEE Transactions on Industrial Electronics*, 45(5):722–729.

Cateriano Yáñez, C., Pangalos, G., and Lichtenberg, G. (2018). An approach to linear state signal shaping by quadratic model predictive control. In *2018 European Control Conference (ECC)*. Accepted.

Emadi, A. (2001). Modelling of power electronic loads in ac distribution systems using the generalized state space averaging method. In *Industrial Electronics Society, 2001. IECON '01. The 27th Annual Conference of the IEEE*, volume 2, pages 1008–1014 vol.2.

Fornberg, B. (1988). Generation of finite difference formulas on arbitrarily spaced grids. *Mathematics of computation*, 51(184):699–706.

Hashim, H. F., Omar, R., and Rasheed, M. (2016). Design and analysis of a three phase series active power filter (SAPF) based on hysteresis controller. In *4th IET Clean Energy and Technology Conference (CEAT 2016)*, pages 1–5.

Kumar, P. and Mishra, M. K. (2016). A comparative study of control theories for realizing APFs in distribution power systems. In *2016 National Power Systems Conference (NPSC)*, pages 1–6.

Liang, X. (2016). Emerging power quality challenges due to integration of renewable energy sources. *IEEE Transactions on Industry Applications*, PP(99):1–1.

Maciejowski, J. (2001). *Predictive control with constraints*. Hemel Hempsted: Prentice Hall/ Pearson Education.

Malesani, L., Mattavelli, P., and Buso, S. (1998). On the applications of active filters to generic loads. In *8th International Conference on Harmonics and Quality of Power. Proceedings (Cat. No.98EX227)*, volume 1, pages 310–319 vol.1.

Mohan, N., Undeland, T. M., and Robbins, W. P. (2003). *Power Electronics. Converters, Applications and Design*. John Wiley and Sons, Inc, third edition.

Shmilovitz, D. (2005). On the definition of total harmonic distortion and its effect on measurement interpretation. *IEEE Transactions on Power Delivery*, 20(1):526–528.

Ziegler, J. G. and Nichols, N. B. (1942). Optimum settings for automatic controllers. *Transactions of the ASME*, 64:759768.

APPENDIX

Model Predictive Control (MPC)

Following the state space dynamics in (2), considering the state reference vector $\mathbf{r} \in \mathbb{R}^n$, the prediction horizon $H_p \in \mathbb{N}$ and the input horizon $H_u \in \mathbb{N}$, the MPC standard quadratic cost function can be formulated, (Maciejowski, 2001)

$$J(k) = \|\mathbf{X}(k) - \Xi(k)\|^2_{\mathbf{Q}} + \|\Delta\mathbf{U}(k)\|^2_{\mathbf{R}} \tag{14}$$

for the optimization problem

$$\min_{\Delta\mathbf{U}(k)} J(k), \tag{15}$$

where $\mathbf{X}(k) \in \mathbb{R}^{H_p n}$ is the future state sequence prediction, $\Xi(k) \in \mathbb{R}^{H_p n}$ the future reference trajectory, and $\Delta\mathbf{U}(k) \in \mathbb{R}^{(H_u+1)m}$ the control input change sequence. Considering with the cost of control error given by the positive semi-definite matrix $\mathbf{Q} \in \mathbb{R}^{H_p n \times H_p n}$ and the cost of control effort by the positive definite matrix $\mathbf{R} \in \mathbb{R}^{(H_u+1)m \times (H_u+1)m}$.

The solution of (15) is given by the optimal control input sequence $\Delta\mathbf{U}^\star(k)$, which is fed to the plant, as shown in the standard MPC control loop of Figure 6.

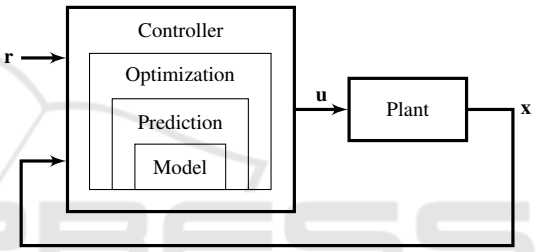

Figure 6: Model Predictive Controller: Classical Scheme.

In order to find the solution $\Delta\mathbf{U}^\star(k)$ in the unconstrained scenario in a numerically well-conditioned manner, the cost function $J(k)$ can be rearranged as

$$J(k) = \left\| \begin{pmatrix} \mathbf{S_Q}(\mathbf{X}(k) - \Xi(k)) \\ \mathbf{S_R}\Delta\mathbf{U}(k) \end{pmatrix} \right\|^2, \tag{16}$$

with the cost matrices factorization

$$\mathbf{Q} = \mathbf{S_Q}^\intercal \mathbf{S_Q}\,, \tag{17}$$

$$\mathbf{R} = \mathbf{S_R}^\intercal \mathbf{S_R}\,, \tag{18}$$

which can be efficiently solved in the least-square sense, e.g. using a QR algorithm, leading to a linear time invariant system controller (Maciejowski, 2001).

Typically the MPC controller uses the receding horizon principle to set an update time strategy for the controlled input signal, where only the first element of the computed optimal input vector sequence $\Delta\mathbf{U}^\star(k)$ is given to the system, then the state values are measured or observed, resp., (Maciejowski, 2001).

Linear State Signal Shaping MPC

A *linear shape class* of a discrete-time state vector signal can be formulated as a kernel representation set

$$\mathcal{X}_{\mathbf{V}} = \{\mathbf{x}(1), \mathbf{x}(2), \ldots | \, \mathbf{V} \begin{pmatrix} \mathbf{x}(k+1) \\ \vdots \\ \mathbf{x}(k+T) \end{pmatrix} = \mathbf{0} \; \forall k = 0, 1, \ldots \}, \quad (19)$$

where the matrix $\mathbf{V} \in \mathbb{R}^{s \times nT}$ defines the behaviour of the state signal shape class, (Cateriano Yáñez et al., 2018).

If a desired behaviour of a dynamical linear system lies in a special signal shape class given by its kernel representation (19), a control algorithm which ensures that state signals are driven to this class belongs to the class of linear MPC problems, (Cateriano Yáñez et al., 2018).

This can be achieved as follows. For $H_p \geq T$, let $\mathbf{V}_j = \mathbf{V}_{:,(j-1)n+1:jn}$, the band matrix

$$\mathbf{P}_V = \begin{pmatrix} \mathbf{V}_1 & \mathbf{V}_2 & \cdots & \mathbf{V}_T & \mathbf{0} & \cdots & \mathbf{0} \\ \mathbf{0} & \mathbf{V}_1 & \mathbf{V}_2 & \cdots & \mathbf{V}_T & \ddots & \vdots \\ \vdots & \ddots & \ddots & \ddots & \ddots & \ddots & \mathbf{0} \\ \mathbf{0} & \cdots & \mathbf{0} & \mathbf{V}_1 & \mathbf{V}_2 & \cdots & \mathbf{V}_T \end{pmatrix} \in \mathbb{R}^{p_1 \times p_2}, \quad (20)$$

with $p_1 = s(H_p - T + 1)$ and $p_2 = nH_p$, can be computed by shifting the shape class matrix $\mathbf{V}$ of (19) for integer multiples of n columns with the help of matrices of zeros $\mathbf{0} = \{0\}^{s \times n}$.

Remark: For $H_p = T$, the matrix $\mathbf{P}_V = \mathbf{V}$ is trivial.

The solution of the MPC optimization problem (15) with reference $\Xi(k) = \mathbf{0}$, weighting matrices $\mathbf{R} = \mathbf{0}$, and $\mathbf{Q} = \mathbf{P}_V{}^{\intercal}\mathbf{P}_V$, leads the state sequence $\mathbf{x}(k+1), \mathbf{x}(k+2), \ldots$ in the shape class given by the matrix $\mathbf{V}$, (Cateriano Yáñez et al., 2018).

Remark: For $\mathbf{R} \neq \mathbf{0}$, The minimum $J(k)$ will rely on a trade off between the cost of control effort introduced by $\mathbf{R}$ and the original cost of control error of not being in the shape class (Cateriano Yáñez et al., 2018).